

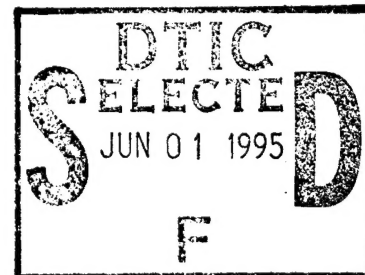
PREDICTION AND MEASUREMENT OF BLADE-VORTEX INTERACTION LOADING

Chee Tung and Judith M. Gallman
U.S. Army Aeroflightdynamics Directorate, ATCOM
NASA Ames Research Center, Moffett Field, Ca., USA

Roland Kube, Wolfgang Wagner, and Berend Van der Wall
Deutsche Forschungsanstalt für Luft- und Raumfahrt
Braunschweig and Goettingen, Germany

Thomas F. Brooks, Casey L. Burley, and D. Douglas Boyd, Jr.
NASA Langley Research Center, Hampton, Va., USA

Gilles Rahier and Philippe Beaumier
Office National D'Etudes et de Recherches Aerospatiales
Chatillon, France



ABSTRACT

An extensive quantity of airload measurements was obtained for a pressure-instrumented model of the BO-105 main rotor for a large number of higher-harmonic control (HHC) settings at Duits-Nederlandse Wind Tunnel (DNW). The wake geometry, vortex strength, and vortex core size were also measured through a laser light sheet technique and LDV. These results are used to verify the BVI airload prediction methodologies developed by AFDD, DLR, NASA Langley, and ONERA. The comparisons show that an accurate prediction of the blade motion and the wake geometry is the most important aspect of the BVI airload predictions.

1 INTRODUCTION

Although the current civil helicopter has been used extensively because of its excellent hover and low speed forward flight capability, the civil helicopter fleet continues to be too noisy for community acceptance, preventing it from reaching its full potential of utilization. One of the major noise sources comes from the rotor blade cutting through its own wake. This phenomenon is known as blade-vortex interaction (BVI). It occurs mostly during descent flight for landing.

Over the last decade, many experimental studies from full-scale flight tests (Refs. 1, 2) to model-scale tests (Refs. 3, 4, 5) have been performed to investigate this BVI phenomenon. It was found that the BVI noise can be scaled (Refs. 6, 7), and expensive flight tests can be simulated by model rotor tests. The development of BVI prediction methodology lagged behind

the experimental studies since no comprehensive rotor code had enough azimuthal (or time) resolution to predict the BVI event. However, several analytical methods (Refs. 8, 9) were developed with limited success as compared with measured blade surface pressure distributions and acoustic signatures. Refs. 8 and 9 indicate that the wake geometry and vortex strength are two major parameters affecting the BVI noise signatures. The information of the wake geometry and vortex strength were not measured in most tests.

An international cooperative test, called the Higher-harmonic-control Aeroacoustic Rotor Test (HART), was conducted by AFDD, DLR, DNW and ONERA at Duits-Nederlandse Wind Tunnel (DNW) to measure not only the blade surface pressure distributions, the blade deformation, and the acoustic signatures, but also the wake geometry using Laser Light Sheet (LLS) technique (Ref. 10) and the vortex strength using Laser Doppler Velocimetry (LDV) method (Refs. 11, 12). The measured data will be used to validate the prediction methodology and to set the future direction for code improvement.

Analytical predictions of BVI events by AFDD, DLR, NASA, and ONERA were performed before the HART test. The predicted wake geometry served as a guide for the LLS and LDV teams to locate the desired vortex. Thus, the wind tunnel simulations of a 6° descent flight case without HHC and two similar cases with HHC are selected for comparison. One is denoted as the baseline case. The second one is the low noise case and the third one is the low vibration case. The results for comparison include the blade flapping motion, elastic deformation, blade surface pressure distribution, sectional lift, and wake geometry at selected azimuthal angles.

This paper is declared a work of the U.S. Government and is not subject to copyright protection in the United States. Presented at the 1st Joint CEAS/AIAA Aeroacoustics Conference, Munich, Germany, June 12-15, 1995

This document has been approved for public release and sale; its distribution is unlimited.

19950531 052

2 PREDICTION METHODOLOGY

Before the HART test, a prediction team, consisting of researchers from US AFDD, German DLR, NASA Langley, and French ONERA was formed. Each member of the prediction team predicted several cases to assist the test team in finding the BVI locations. The prediction methodology developed by each organization has been discussed in detail (Ref. 9). A brief description of each prediction method is given in the following.

To predict the blade loading, AFDD uses a comprehensive analytical model of rotor aerodynamics and dynamics (CAMRAD/JA) to determine the vortex trajectory, vortex strength and blade partial inflow angles. This information is then used as an input to FPR, a 3-D, unsteady full potential code, to determine the aerodynamic surface pressures. Similarly, DLR uses the S4 code which consists of three modules; namely, an unsteady aerodynamic model, a wake model, and an aeroelastic model. These three models are controlled by the rotor trim algorithm. The aerodynamic model is a lifting line method with the Leiss dynamic stall algorithm. The wake model uses a prescribed and distorted wake developed by T. Beddoes (Ref. 13). Uncoupled flap, lead-lag, and torsional modes are used. At NASA Langley, a comprehensive rotor code CAMRAD.MOD1 and HIREs or a full-potential CFD code, FPRBVI are used for the blade load prediction. The numerical methods developed at ONERA combine R85 and METAR codes to get the trim solution, MESIR/MENTHE to calculate the wake geometry and ARHIS to obtain the blade loading.

Selected pre-test predictions will be discussed and compared with post-test predictions. The post-test prediction results from the modification of some of the parameters in the prediction codes.

3 EXPERIMENTAL DATA

The test data used here for comparison were obtained in the DNW (Refs. 14, 15). The model is a forty percent Mach scaled model of a hingeless BO-105 main rotor. The blades are well instrumented and one blade was installed with 124 miniature pressure transducers and 32 strain gauges. The blade pressure and strain gauge signals were recorded at a rate of 2048/Rev. An average of 64 revolutions was sampled for each rotor condition and HHC. The rotor performance data were measured at a rate of 128 per revolution over a period of 32 revolutions. The wake geometry and vortex strength were measured by the LLS and LDV techniques respectively.

Three cases are selected for comparison. One is the baseline case (Run 140) without HHC. The second case (Run 138) produces lower noise with 3/Rev HHC (0.8° amplitude and 300° phase angle) and the third one produces (Run 133) lower vibration with 3/Rev HHC

(0.8° amplitude and 180° phase angle). Other flight parameters are:

Advance ratio: $\mu = 0.15$

Tip Mach number: $M_H = 0.641$

Shaft angle: $\alpha_s = 5.3^\circ$

Thrust coefficient: $C_T = 0.0044$.

4 RESULTS AND DISCUSSIONS

4.1 Pre-test Predictions

Before the test entry at DNW, each organization calculated several selected test cases with different HHC settings and shaft angles. These results were used as a guide to identify the BVI location for LLS flow visualization and LDV measurements as well as a sanity check for the pressure data. Although there are extensive results available for comparison, only the predicted sectional lift coefficients for the above mentioned three cases are presented here. Fig. 1 shows the comparison of the sectional lift coefficients at $r/R = 0.87$ for the baseline, low noise and low vibration case respectively. For the baseline case (Run 140), there are eight BVI interactions on the advancing side and five on the retreating side. For the low noise case (Run 138), only two dominant BVI occurs on the advancing side and three on the retreating side. The 2/Rev and 3/Rev loadings which will affect the low frequency component of the radiated noise are best predicted by ONERA. Langley's calculation shows the correct number of interactions on both the advancing and the retreating sides with higher magnitude than the test data. It indicates that the predicted miss-distance between the blade and the vortex is probably closer than the actual one. The effect of blade dynamics on the blade BVI loading has been discussed in Ref. 9.

4.2 Post-test Predictions

After the test was completed, each organization researched possible improvement to the prediction. Since the dynamic model required improvements to match the basic 2/Rev or 3/Rev loadings, AFDD modified the blade elastic properties at the blade root sections and used the flutter analysis in CAMRAD/JA to match the measured first two flapping modes, first two torsion modes, and first lead-lag mode. DLR attempted to improve their prescribed wake model by (1) the measured vortex core radius from the test, (2) a wake contraction of 15 percent, (3) adjusting the wake orientation with respect to the blade tip path plane to match the measured vortex miss-distance, and (4) a dual vortex pair consisting of a clockwise and a counterclockwise rotating vortex. NASA Langley implemented the measured blade motion (flapping, torsion, and lead-lag) into CAMRAD.Mod 1 code. ONERA used a measured vortex core size for their calculations. The new results are compared with the test data.

4.3 Tip Deflection and Elastic Pitch

The predicted tip deflections are plotted against the measured results in Fig. 2. Both DLR and ONERA results show a reasonable agreement with test data for all three cases while AFDD predictions do not have the 2/Rev or 3/Rev shape even when the modified structural properties are used. It should be noticed that the difference of the tip deflection for low noise case at $\psi = 50^\circ$, where the blade encounters the vortex, and $\psi = 150^\circ$, where the vortex is generated, is greater than the one of baseline case. This indicates that the miss-distance between the blade and the vortex increases for the low noise case. As for the elastic pitch at $\psi = 60^\circ$ for all three cases in Fig. 2, most predictions are over-estimated as compared with the test data derived from the measured strain gauges. NASA Langley uses the measured blade motion as an input to CAMRAD.Mod 1 code, so the results match the test data.

4.4 BVI Locations (Top View)

From the leading-edge pressure measurements along the rotor span, one may use the valley/peak at each advancing and retreating side to identify the measured BVI locations (Ref. 16). The comparison between the predicted and measured BVI locations is shown in Fig. 3. For the baseline case (Run 140), the measured BVI locations (open symbol) occur in the first and fourth quadrants. The measured BVI locations near $\psi = 0^\circ$ seem to be parallel to the flow. It is the interaction of the vortex with the rotor hub that causes the distortion of the wake. For the low noise case (Run 138), the measured BVI locations are clustered near $\psi = 15^\circ$, $\psi = 90^\circ$, and $\psi = 285^\circ$. As for the low vibration case (Run 133), the measured BVI locations occur near $\psi = 60^\circ$ and $\psi = 300^\circ$. Only a part of the predicted BVI locations (solid symbol) among each organization and for all three cases agrees well with the measured ones. The difference in the top view of the BVI locations affects the phase shift in the sectional loadings. A fifteen percent wake contraction used by DLR gives a quite different BVI location near $\psi = 90^\circ$ and $\psi = 270^\circ$ as compared other predictions.

4.5 Wake Geometry

The pre-test predicted wake geometry and the measured pressure data were used to identify the most important blade-vortex interactions. However, the wake geometry was measured before the actual BVI because the wake will be obscured by the blade. Selected vortex wake segments (only the tip vortices are presented) at $\psi = 35^\circ$ and $\psi = 295^\circ$ for all three cases are compared with the test data obtained from LLS technique. Fig. 4 shows both the top and side view of the wake geometry. All the vertical coordinates of the wake geometry are relative to the blade tip. No exact blade position is shown in Fig. 4, but the blade is close to a horizontal straight line at $z = 0$. For the baseline case,

the miss-distance prediction (open symbol) of vortices number 5 and 6, from each organization agrees well with the measurements (solid symbol) on both the advancing and retreating sides, but the top view shows that the interactions occur at different azimuthal angles. The measured vortex segments were produced at azimuthal angles from about $\psi = 120^\circ$ to $\psi = 150^\circ$. For the low noise case, the miss-distance at $\psi = 35^\circ$ is larger compared with the one of the baseline case. It implies that the BVI loading is relatively weaker. Most predictions show an increase in miss-distance. For the low vibration case, the blade produces negative loadings near the outboard sections. It also produces two trailing vortices of opposite sign. One is clockwise (solid symbol with solid line) and the other is counterclockwise (solid symbol and dash line). None of the analyses predict this phenomenon at the present time. However, a new wake modeling by ONERA that deals with the multiple wake roll-up will be presented in another paper.

4.6 Sectional Loads

The improved predictions of the sectional lift coefficients for all three cases at $r/R = 0.75, 0.87$, and 0.97 are shown in Fig. 5. Predicted sectional loadings by AFDD show no significant improvement over the pre-test results. They do not produce the 2/Rev loading for the baseline case and the 3/Rev loading for the other two cases. The post-test predictions by DLR do show a great improvement at the inboard sections for all three cases. However, there exist two loading spikes near $\psi = 90^\circ$ and $\psi = 270^\circ$ at $r/R = 0.97$. These two spikes may be caused by the fifteen percent wake contraction that causes the wake to move inboard and produces a large upwash outboard. The adjustment of the wake orientation also reduces the BVI peak-to-peak loadings for some cases. The new results predicted by NASA Langley are in better agreement with test data even though some of the 2/Rev and 3/Rev loadings are over-estimated. This shows that the airloads depend strongly upon the blade motion. ONERA's results using the measured vortex core size show a marginal improvement (some of the BVI peak-to-peak values are reduced) over the already good pre-test results.

5 CONCLUDING REMARKS

The pre-test results were useful during the test to locate the important BVI events and to reduce some of the runs in the test matrix. The HART test data show that BVI noise can be reduced with HHC (Run138). For this case, the miss-distance between the blade and the vortex wake was increased by twice the value of the baseline case (Run140). The change in miss-distance is the major factor in reducing the BVI noise. Based on this fact, several alternate ideas were used to improve the prediction. The wake geometry is improved by prescribing the motion of the blade and this appears to be the most important factor in obtaining better cor-

	<input checked="" type="checkbox"/>
	<input type="checkbox"/>
	<input type="checkbox"/>
Codes	
1/ or	
acial	
A-1	

relation with the data. Other parameters such as the blade structural properties, the vortex core size, and the wake orientation seem to be less important. The comparison of four different BVI prediction methodologies with the HART test data indicates that accurate predictions require further improvements in wake modeling.

6 ACKNOWLEDGMENTS

The authors would like to express their appreciation to Mr. Scott Low for his work on all the graphics.

7 REFERENCES

- [1] Sakowsky, P. C. and Charles, B. D., "Noise Measurement Test Results for AH-1G Operational Loads Survey", Vols I and II, Bell Helicopter Co. Report 299-099-831, Oct. 1976.
- [2] Boxwell, D. A. and Schmitz, F. H., "Full-Scale Measurements of Blade-Vortex Interaction Noise", presented at the 36th Annual National Forum of the American Helicopter Society, Washington, D. C., May 1980.
- [3] Boxwell, D. A., Schmitz, F. H., Spletstoesser, W. R., and Schultz, K. J., "Model Helicopter Rotor High-speed Impulsive Noise: Measured Acoustics and Blade Pressures", presented at the 9th European Rotorcraft Forum, Paper No.17, Stressa, Italy, Sept. 1983.
- [4] Dadone, L. U., Caradonna, F. X., Ramachandra, K., Silva, M. J., and Poling, D., "The prediction of Loads on the Beoing Helicopters Model 360 Rotor", presented at the 45th Annual National Forum of the American Helicopter Society, Boston, MA, May 1989.
- [5] Lorber, P. F., "Aerodynamic Results of a Pressure-Instrumented Model Rotor Test at the DNW", presented at the 46th Annual National Forum of the American Helicopter Society, Washington D. C., May 1990.
- [6] Schmitz, F. H., Boxwell, D. A., Lewy, S., and Dahan, C., "A Note on the General Scaling of Helicopter Blade-Vortex Interaction Noise", presented at 38th Annual National Forum of the American Helicopter Society, Anaheim, California, May 1982.
- [7] Boxwell, D. A., Schmitz, F. H., Spletstoesser, W. R., and Schultz, K. J., "Helicopter Model Rotor Blade Vortex Interaction Impulsive Noise : Scalability and Parametric Variations," Journal of American Helicopter Society, Vol. 32, No. 1, January 1987.
- [8] Yu, Y. H., Tung, C., Gallman, J., spletstoesser, W. R., Schultz, K. J., Spiegel, P., Rahier, G., and Michea, B., "Aerodynamics and Acoustics of Rotor Blade-Vortex Interactions: Analysis Capability and its Validation", presented at 15th AIAA Aeroacoustics Conference, Long Beach, CA, Oct. 1993.
- [9] Beaumier, P., Prieur, J., Rahier, G., Demargne, Tung, C., Gallman, J. M., Yu, Y. H., Kube, R., Van der Wall, B. G., Schultz, K. J., Spletstoesser, W. R., Brooks, T. F., Burley, C. L., and Boyd, D. D., "Effect of Higher Harmonic Control on Helicopter Rotor Blade-Vortex Interaction Noise and Initial Validation", AGARD Meeting, Berlin, Germany, Oct. 11-14, 1994.
- [10] Mercker, E. and Pengel, K., "Flow Visualization of Helicopter Blade Tip Vortices", presented at 18th European Rotorcraft Forum, Avignon, France, Sept. 1992.
- [11] Seelhorst, U., Butefisch, K. A., and Sauerland, K. H., "Three Component Laser-Doppler-Velocimeter Development for Large Wind Tunnel", in ICIASF 1993 Record, pp33.1-33.7, 1993.
- [12] Boutier, A., Lafevre, J., Soulevant, D., and Dunand, F., "2D Laser Velocimetry near Helicopter Blades in DNW (NLR)", in ICIASF 1993 Record, pp32.1-32.8, 1993.
- [13] Beddoes, T. S., "A wake Model for High Resolution Airlods", US Army/AHS International Conference on Rotorcraft Basic Research, Research Triangle Park, NC, February 1985.
- [14] Yu, Y. H., Gmelin, B., Heller, H., Philippe, J. J., Mercker, E., and Preisser, J. S., "HHC Aeroacoustics Rotor Test at the DNW - The Joint German/French/US HART Project" Presented at 20th European Rotorcraft Forum at Amsterdam, the Netherlands, Oct. 1994.
- [15] Kube, R., Spletterstoesser, W. R., Wagner, W., Seelhorst, U., Yu, Y. H., Boutier, A., Michali, F., and Mercker, E., "Initial Results from the Higher Harmonic Control Aeroacoustic Rotor Test (HART) in the German-Dutch Wind Tunnel", presented at the 75th AGARD Fluid Dynamics Panel Meeting on Aerodynamics and Aeroacoustics of Rotorcraft, Berlin, Germany, Oct. 1994.
- [16] Caradonna, F. X., Laub, G. H., and Tung, C., "An Experimental Investigation of the Parallel Blade-Vortex Interaction", presented at 10th European Rotorcraft Forum, the Hague, the Netherlands, August, 1984.

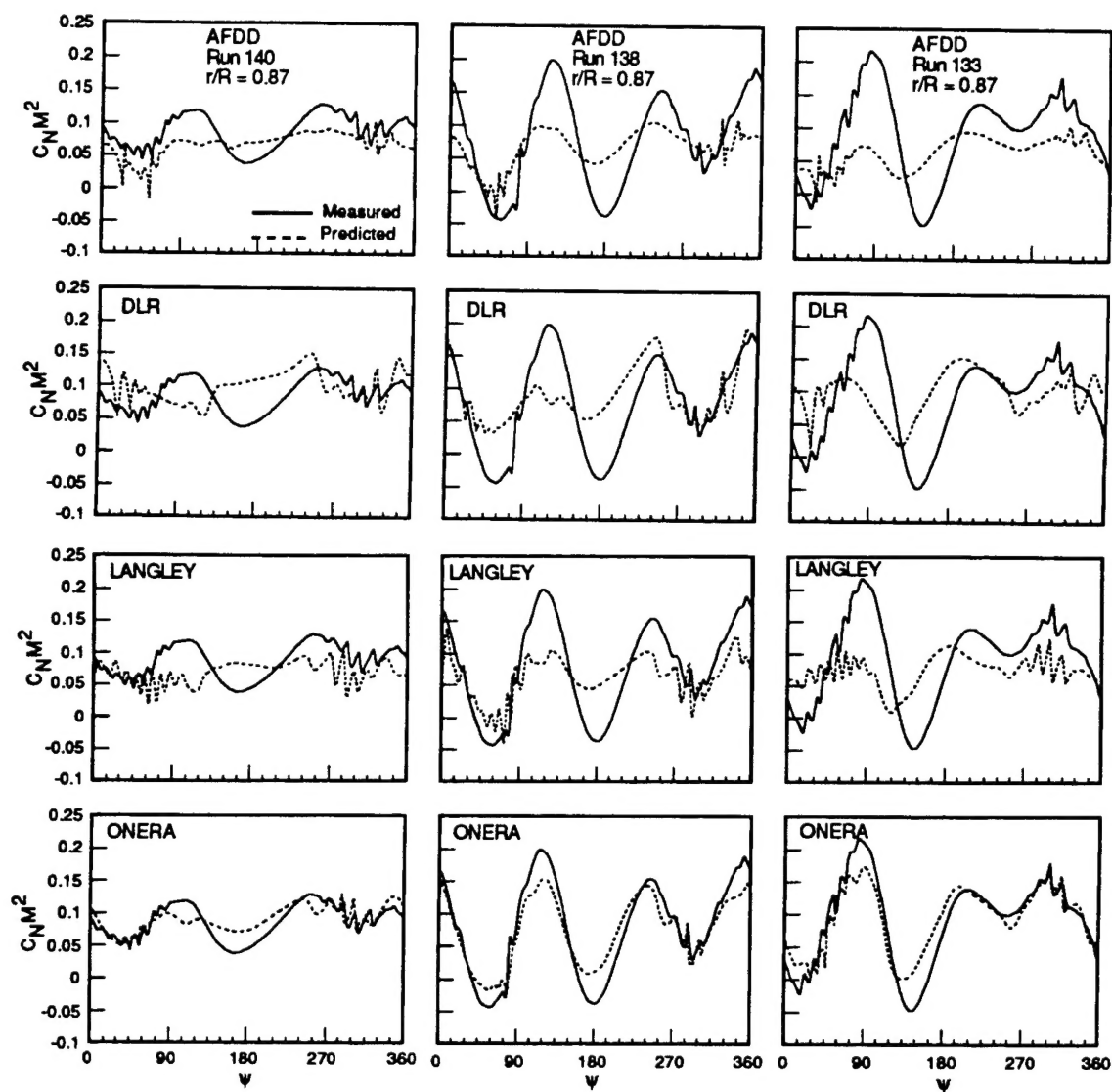


Fig. 1 Comparison of pre-test loading predictions at $r/R = 0.87$ with test data.

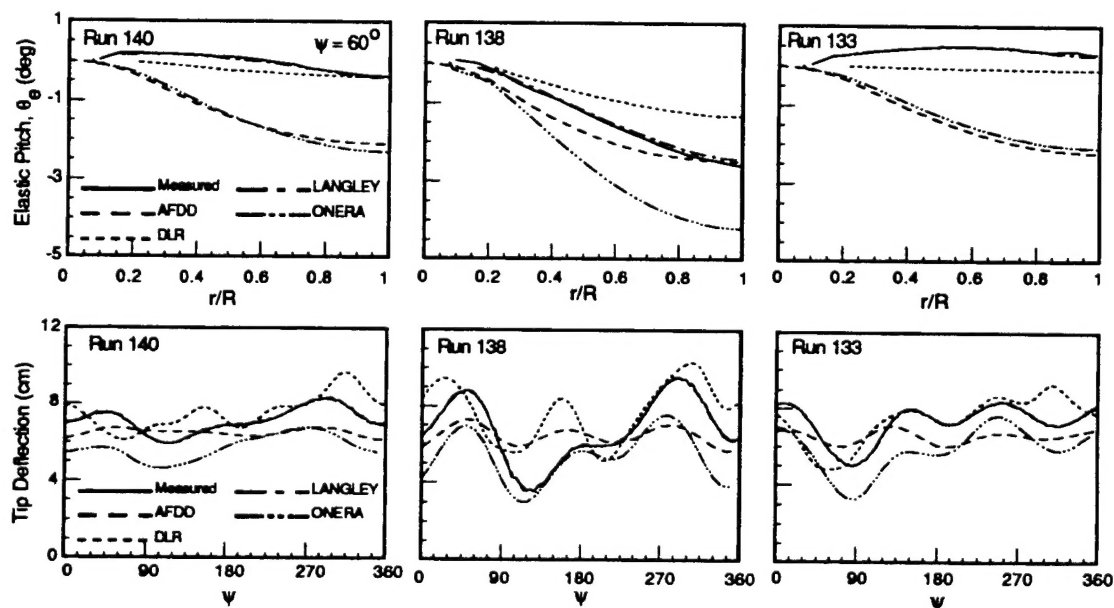


Fig. 2 Comparison of elastic pitch at $\psi = 60$ degrees and tip deflection with test data.

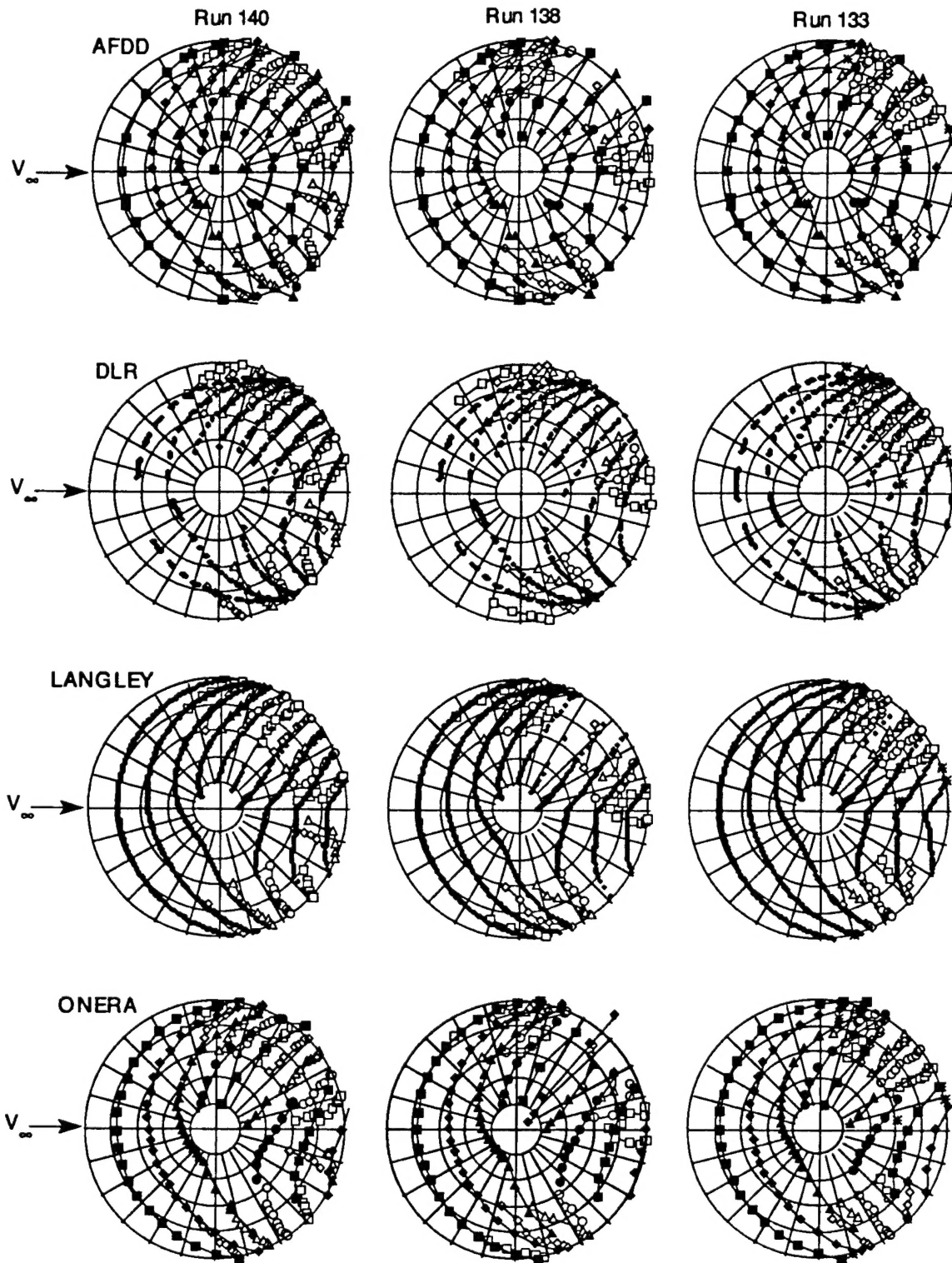


Fig. 3 Comparison of BVI locations (top view) with data derived from measured leading-edge pressure.

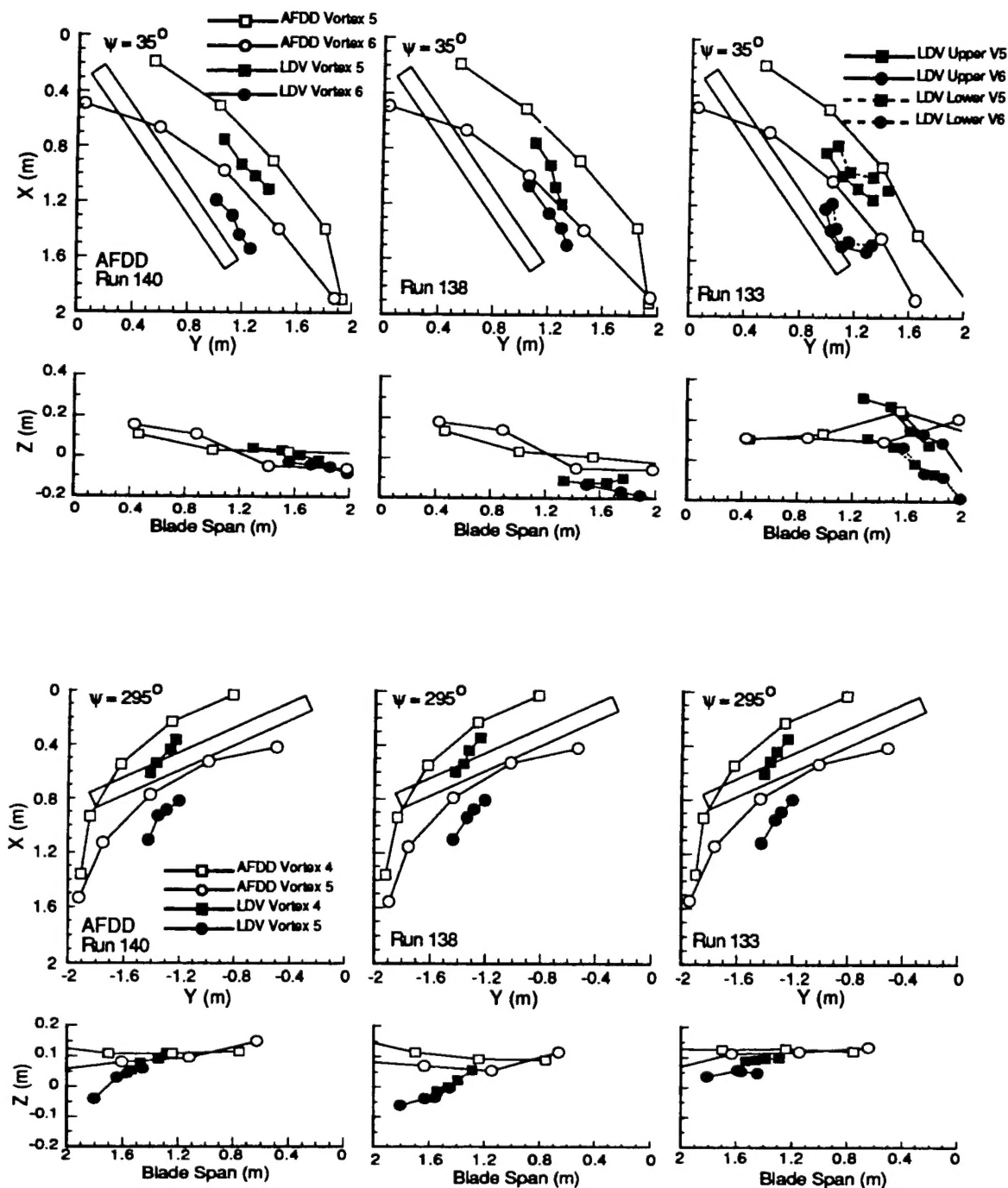


Fig. 4 Comparison of measured and predicted vortex segments at $\psi = 35$ degrees and $\psi = 295$ degrees.

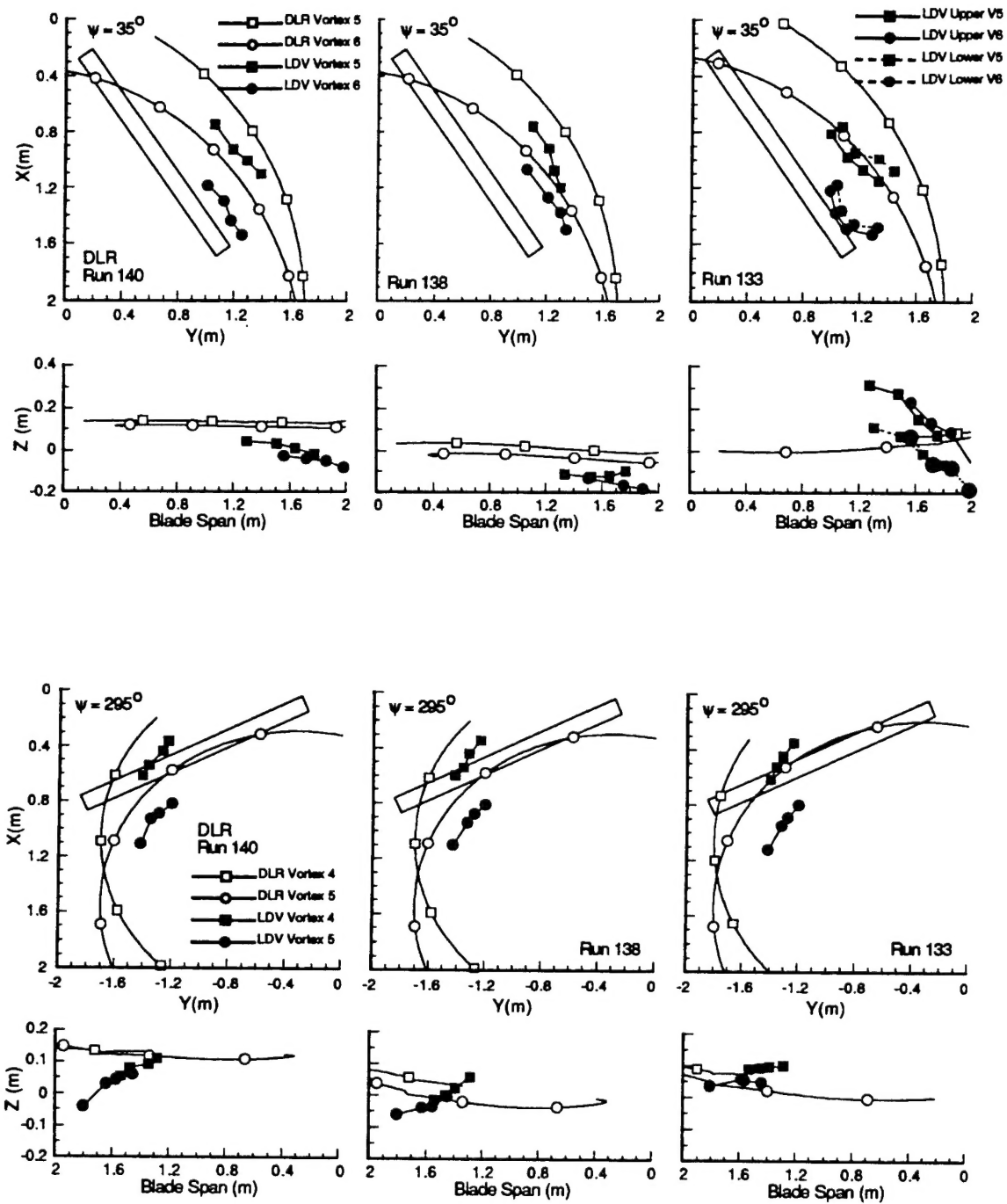


Fig. 4 (continued) Comparison of measured and predicted vortex segments at $\psi = 35$ degrees and $\psi = 295$ degrees.

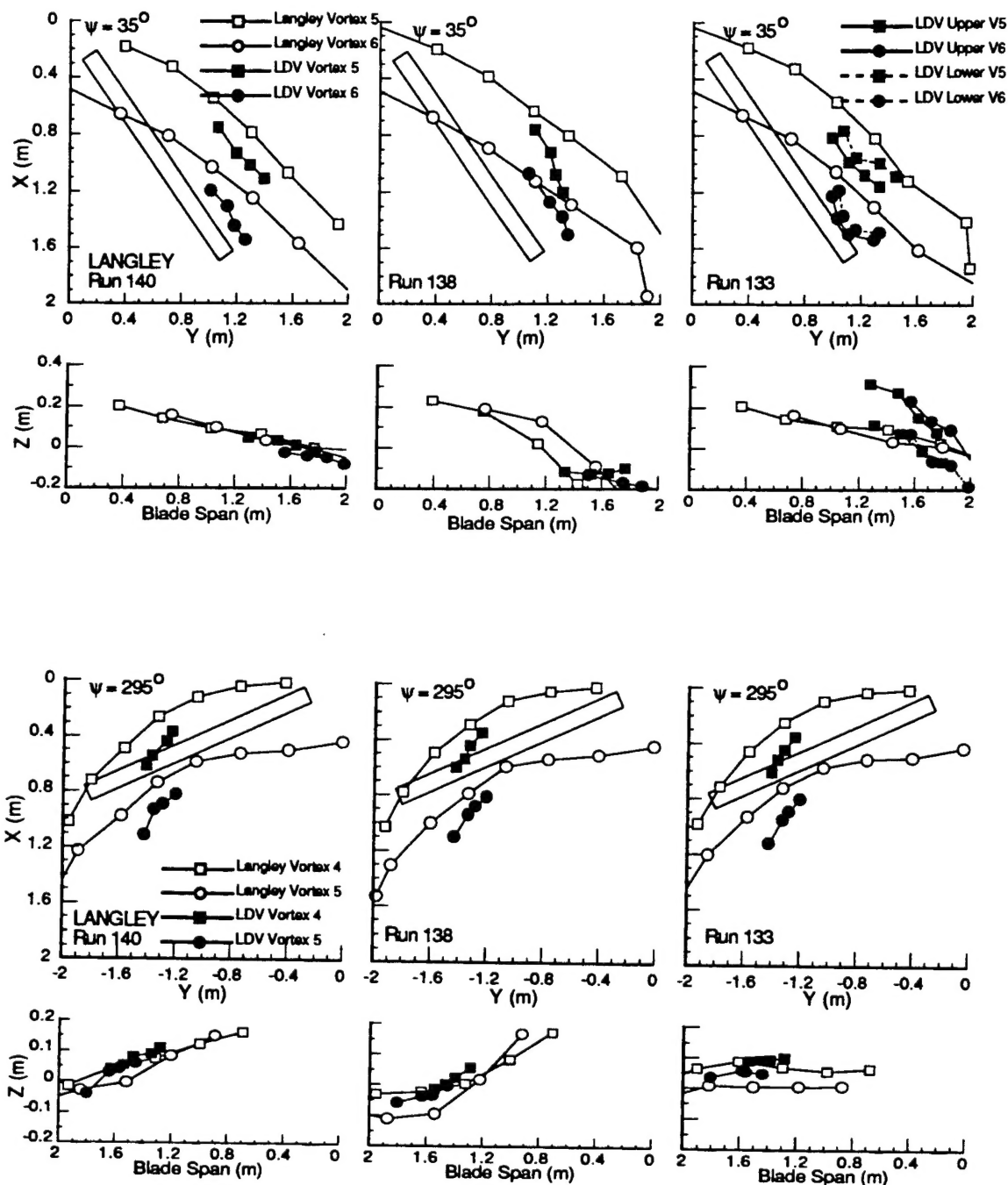


Fig. 4 (continued) Comparison of measured and predicted vortex segments at $\psi = 35$ degrees and $\psi = 295$ degrees.

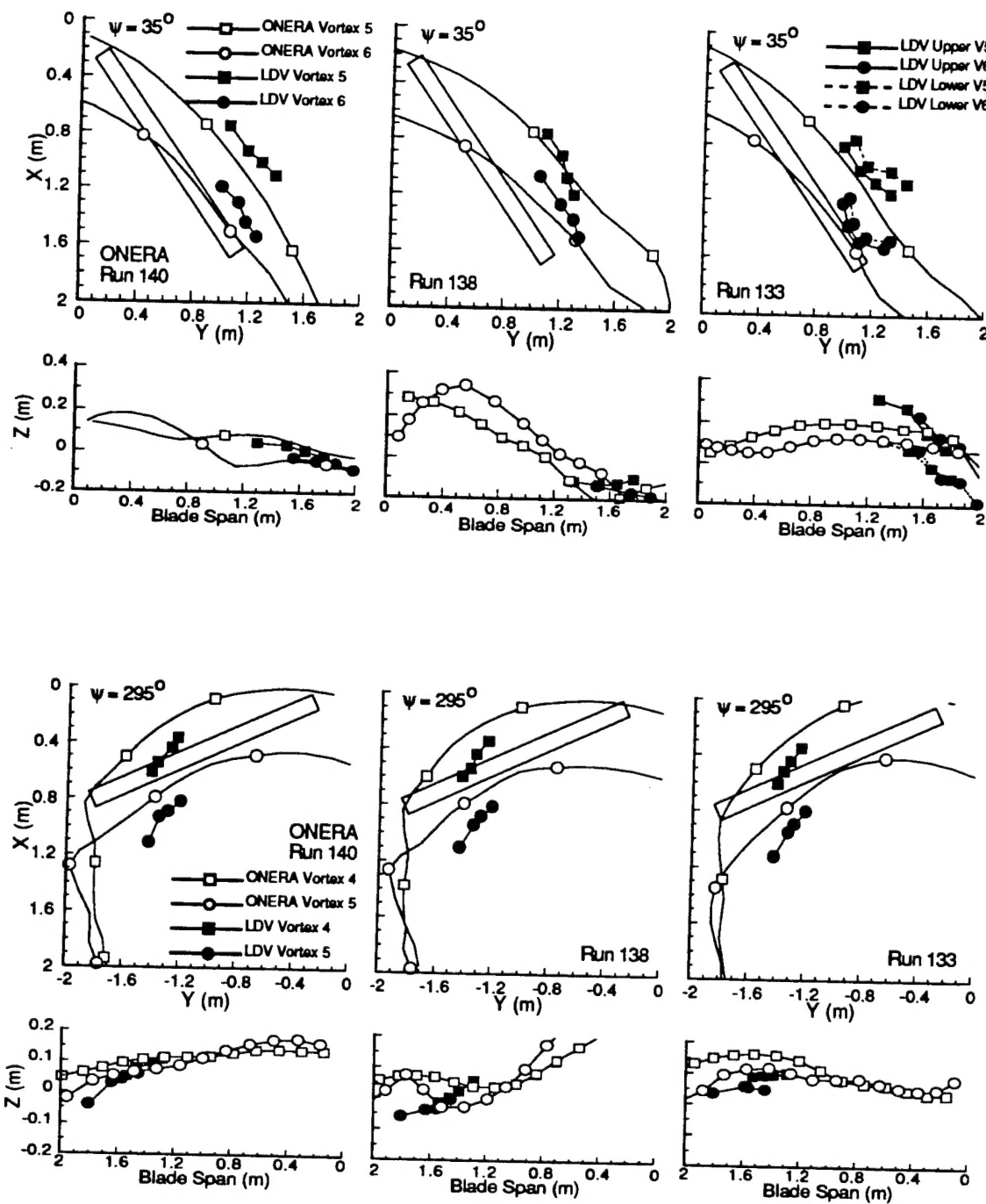


Fig. 4 (continued) Comparison of measured and predicted vortex segments at $\psi = 35$ degrees and $\psi = 295$ degrees.

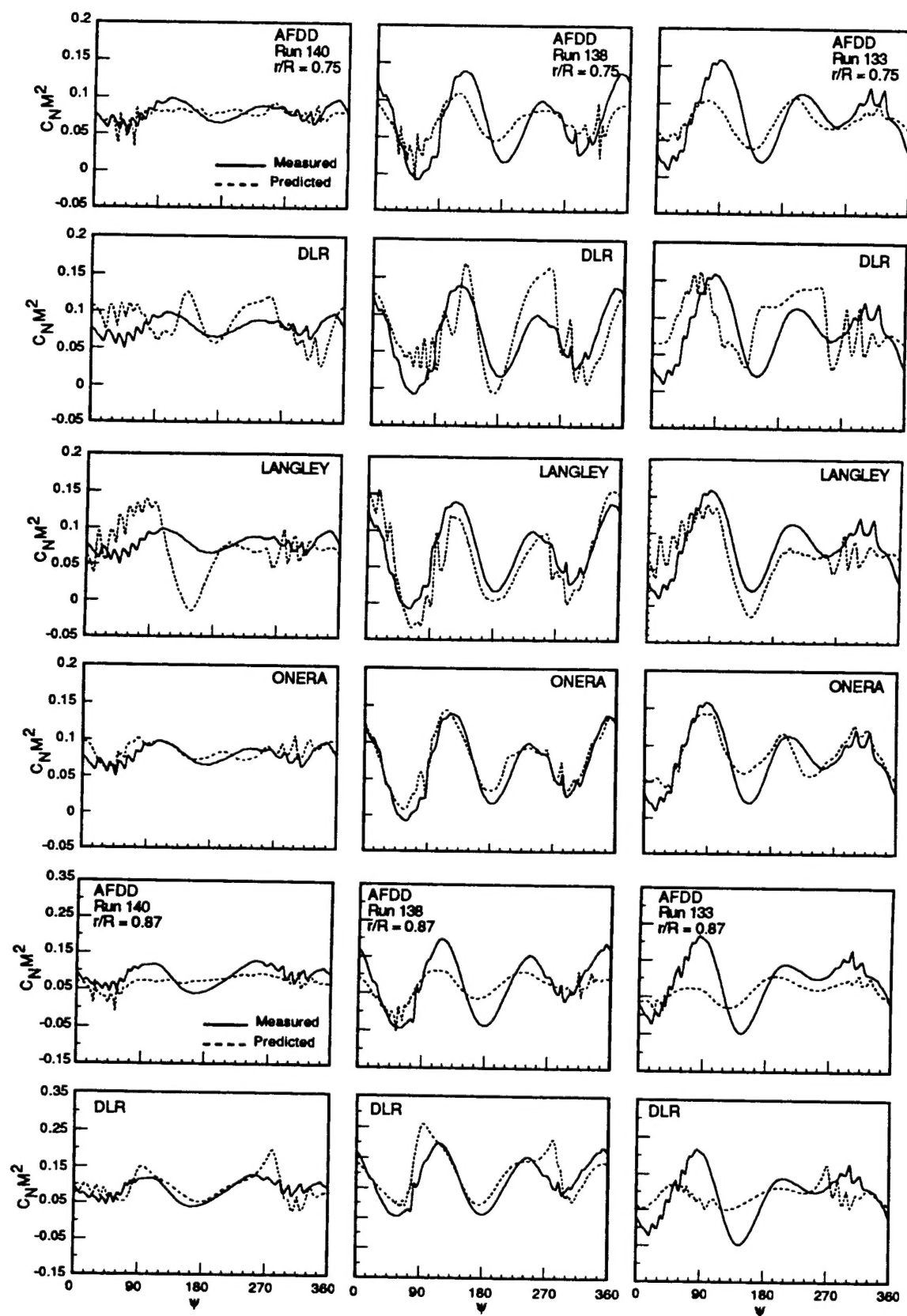


Fig. 5 Comparison of post-test loading predictions at $r/R = 0.75$, $r/R = 0.87$, and $r/R = 0.97$ with test data.

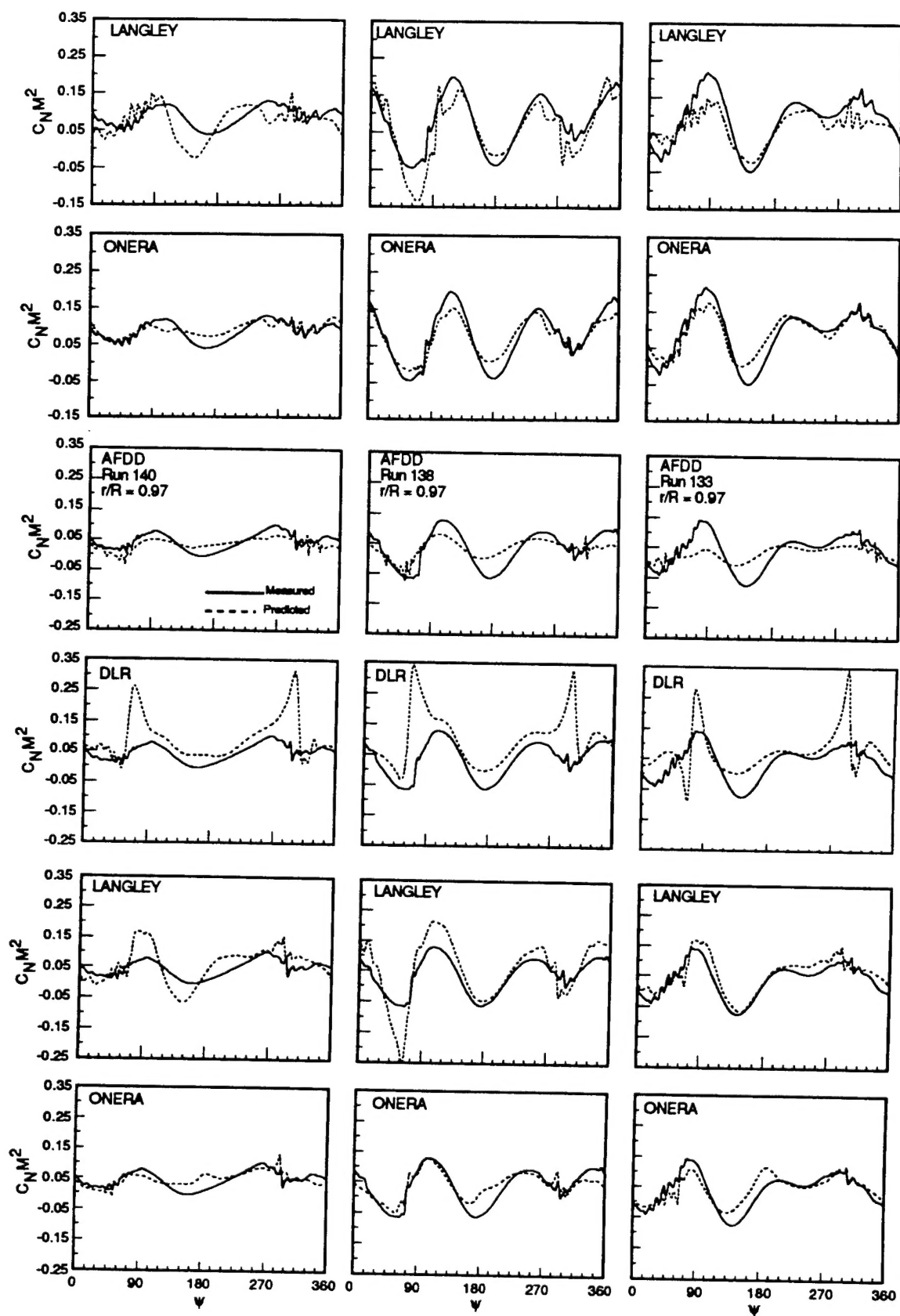


Fig. 5 (continued) Comparison of post-test loading predictions at $r/R = 0.75$, $r/R = 0.87$, and $r/R = 0.97$ with test data.